J Neurophysiol 120: 105–114, 2018.
First published March 28, 2018; doi:10.1152/jn.00911.2017.

RESEARCH ARTICLE | *Sensory Processing*

Gap encoding by parvalbumin-expressing interneurons in auditory cortex

Clifford H. Keller, Katherine Kaylegian, and Michael Wehr
Institute of Neuroscience, University of Oregon, Eugene, Oregon

Submitted 20 December 2017; accepted in final form 26 March 2018

Keller CH, Kaylegian K, Wehr M. Gap encoding by parvalbumin-expressing interneurons in auditory cortex. *J Neurophysiol* 120: 105–114, 2018. First published March 28, 2018; doi:10.1152/jn.00911.2017.—Synaptic inhibition shapes the temporal processing of sounds in auditory cortex, but the contribution of specific inhibitory cell types to temporal processing remains unclear. We recorded from parvalbumin-expressing (PV+) interneurons in auditory cortex to determine how they encode gaps in noise, a model of temporal processing more generally. We found that PV+ cells had stronger and more prevalent on-responses, off-responses, and postresponse suppression compared with presumed pyramidal cells. We summarize this pattern of differences as "deeper modulation" of gap responses in PV+ cells. Response latencies were also markedly faster for PV+ cells. We found a similar pattern of deeper modulation and faster latencies for responses to white noise bursts, suggesting that these are general properties of on- and off-responses in PV+ cells rather than specific features of gap encoding. These findings are consistent with a role for PV+ cells in providing dynamic gain control by pooling local activity.

NEW & NOTEWORTHY We found that parvalbumin-expressing (PV+) interneurons in auditory cortex showed more deeply modulated responses to both gaps in noise and bursts of noise, suggesting that they are optimized for the rapid detection of stimulus transients.

auditory cortex; gap detection; inhibition; optogenetics; temporal processing

INTRODUCTION

A fundamental task faced by the auditory system is the temporal processing of dynamic acoustic streams such as music and speech. Age-related speech processing deficits affect more than half of the population over 65. These speech processing deficits can occur even with completely normal audiometric hearing and are instead associated with temporal processing deficits in the central auditory system (Ben-David et al. 2011; Helfer and Vargo 2009; Walton 2010). Temporal processing deficits are also correlated with developmental deficits in language and reading comprehension (Tallal et al. 1985). Age-related loss of synaptic inhibition occurs at multiple levels of the auditory system, including the cochlear nuclei, inferior colliculus (IC), and auditory cortex (Caspary et al. 2008). This loss of inhibition is thought to be involved in temporal processing deficits (Caspary et al. 2008), but how inhibitory circuits contribute to temporal processing remains unclear.

Address for reprint requests and other correspondence: M. Wehr, Institute of Neuroscience, 1254 University of Oregon, Eugene, OR 97403 (e-mail: wehr@uoregon.edu).

Gap detection, the rapid detection of brief gaps in background noise, is a well-established model for temporal acuity, such as that required for phoneme discrimination. Age-related gap detection deficits are well correlated with speech comprehension deficits (Fitzgibbons and Gordon-Salant 1996; Glasberget al. 1987; Schneider et al. 1994; Snell and Frisina 2000). Inhibitory circuits in auditory cortex are clearly involved in gap detection, because optogenetic manipulation of either parvalbumin-expressing (PV+) or somatostatin-expressing interneurons enhances or impairs gap detection, depending on the sign and the timing of the manipulation (Weible et al. 2014a, 2014b). Yet, it remains unclear precisely how inhibition shapes cortical activity during gap detection and whether specific inhibitory cell types have distinct roles in gap detection or temporal processing in general. No one has recorded from inhibitory interneurons during gap detection, so it is unknown whether or how they respond to gaps.

How might inhibitory interneurons contribute to temporal processing in auditory cortex? In this study we focus on PV+ cells, the most prevalent class of cortical interneurons. PV+ cells appear to pool local excitatory synaptic input rather indiscriminately, which tends to broaden their tuning for stimulus features compared with pyramidal neurons (Hofer et al. 2011; Kerlin et al. 2010; Moore and Wehr 2013). PV+ cells also make fast, powerful synapses onto the soma, proximal dendrites, and axons of pyramidal neurons. These properties of both their input and output connectivity make PV+ cells likely candidates to provide cortical gain control. Cortical synaptic inhibition also has been shown to sharpen spike timing (Wehr and Zador 2003), which could improve temporal acuity by enhancing the temporal precision of gap encoding. Inhibition also has been proposed to shape gap responses by implementing a temporal comparison between ongoing and recent activity (Weible et al. 2014b). Finally, if PV+ cells are tuned for specific gap durations, they could confer gap duration tuning to pyramidal cells by suppressing responses away from the target cell's preferred gap duration. To examine these possible roles, we recorded from cortical PV+ inhibitory interneurons in auditory cortex to characterize how they encode gaps and thereby contribute to temporal acuity.

METHODS

All procedures were in accordance with the National Institutes of Health guidelines, as approved by the University of Oregon Institutional Animal Care and Use Committee.

Mice. We used optogenetic tagging to identify parvalbumin-positive interneurons that expressed channelrhodopsin2 (ChR2) and re-

sponded to light (Lima et al. 2009; Moore and Wehr 2013). All mice were 7–12 wk of age at the time of surgery (and 10–15 wk at the conclusion of recordings) and were bred to the C57Bl6/J background strain. We used offspring ($n = 9$ total, $n = 3$ males, 4 females, 2 unknown) of a cross between homozygous Pvalb-IRES-Cre ("PV"; stock no. 008069; The Jackson Laboratory) and homozygous CAG-ChR2-eYFP lines ("ChR2"; stock no. 012569, line Ai32; The Jackson Laboratory). In these mice (PV × ChR2), ChR2 was expressed in PV+ interneurons, with 97% specificity (Moore and Wehr 2013). All mice had normal startle responses and behavioral gap detection and showed no evidence of C57BL/6J age-related hearing loss, which is generally not seen until after 12 wk of age (Ison et al. 2007).

Surgery. We implanted mice with an array of eight tetrodes for recording as well as an optic fiber for laser activation of PV+ interneurons. We administered dexamethasone (0.1 mg/kg) and atropine (0.03 mg/kg) preoperatively to reduce inflammation and respiratory irregularities. Surgical anesthesia was maintained with isoflurane (1.25–2.0%). The tetrode array was inserted vertically through a small craniotomy (2 mm × 1 mm) dorsal to the left auditory cortex and cemented into place with Grip Cement (Dentsply, Milford, DE). For optogenetic excitation, a single 200-μm optic fiber was implanted overlying auditory cortex. A thin coating of antibacterial ointment was applied over the dura, and the whole area was covered with Grip Cement. Ketoprofen (4.0 mg/kg) was administered postoperatively to minimize discomfort. Mice were housed individually after the surgery and allowed 7 days of postoperative recovery.

Stimulus delivery and data acquisition. All data were collected in a sound-attenuating chamber. Mice were allowed to freely move about within a 15-cm-diameter plastic arena with mouse litter covering the floor. Sounds were delivered from a free-field speaker directly above the animal. The speaker was calibrated to within ±1 dB using a Brüel and Kjær type 4939 1/4-in. microphone positioned horizontally in the center of the arena at a height of 2 cm above the arena floor (mouse ear height), without the animal present. Sound intensity varied by no more than 8.5 dB at different positions around the arena floor. To identify PV+ interneurons, we presented pulses of blue light (duration 100 ms, wavelength 445 nm, total power 5–30 mW, corresponding to 160–950 mW/mm^2 irradiance measured at the fiber tip). Pulses were presented interleaved with 50-ms white noise (WN) bursts and silent periods with an intertrial interval of 500 ms. We then tested responses to WN bursts of various durations (1–256 ms) at 70 dB SPL. WN bursts were presented every 1,000 ms in random order and repeated 10–30 times. To test responses to gaps, silent gaps of duration 1–256 ms were inserted into continuous background white noise (80 dB SPL). Each gap duration was presented in random order, 15–30 repetitions, separated by an intertrial interval of 1 s. Sound onsets and offsets for WN bursts and gap stimuli (including gap onsets and terminations) had rise and fall times of zero. Note that this did not introduce any spectral splatter because of the white noise carrier.

Single-neuron recording. We implanted an array of 8 tetrodes passed through a 1 × 4 array of 28-gauge stainless steel hypodermic tubing, with 2 tetrodes per tube. Tetrodes were made of 18-μm (25 μm coated) tungsten wire (California Fine Wire). The entire array was mounted on a custom microdrive. Tetrode data were acquired with 32-channel RHD2000 hardware (Intan Technologies) and Open Ephys software (https://www.open-ephys.org). A minimum threshold of 50 μV was set for collection of spiking activity. Spiking activity of individual neurons was isolated offline using the open source spike sorting software packages Simpleclust (https://jvoigts.scripts.mit.edu/blog/simpleclust-manual-spike-sorting-in-matlab) and MClust (https://redishlab.neuroscience.umn.edu/MClust/MClust.html). Measures of peak and trough waveform voltage, total energy, and first principal component were used as waveform separation parameters in two-dimensional (2-D) cluster space. Cells were accepted for analysis only if they had a cluster boundary completely separate from adjacent cluster boundaries, and completely above threshold, on at least one 2-D view.

Data analysis and statistics. We characterized neuronal responses to laser pulses, white noise stimuli, and gap-in-noise stimuli. Spike width was measured from 20% of the peak to 20% of the trough (Fig. 1*D*, *inset*). Latencies to the half-maximum stimulus-evoked firing rate were calculated from peristimulus histograms (PSTHs) of spike times accumulated by repeated presentation of WN bursts or gaps in noise and smoothed by convolution with a Gaussian ($\sigma = 6$ ms), as described in Moore and Wehr (2013). Population-averaged PSTHs across cells for each stimulus were obtained from the baseline-subtracted PSTHs after normalization to the maximum firing rate for that cell across all stimuli. For comparison between responses to stimuli of differing durations, we binned spiking data at 5 ms. We quantified excitatory responses as the spike count in a 50-ms window immediately following sound onset or sound offset, and we quantified suppressive responses in a window from 70 to 140 ms after onset or offset. Note that for short gaps these time periods overlap, which provides information about temporally overlapping responses to sound offset and onset. We tested for significant gap responses using a paired *t*-test, comparing spike counts during a given response window to spike counts on interleaved trials without a gap. Similarly, we tested for significant WN responses using a paired *t*-test, comparing spike counts during a given response window to spike counts in a silent window of the same duration before the stimulus. A cell was only considered to have a response if the same sign of significant change occurred for two consecutive durations. For example, a cell with a significant excitatory response to the onset of a 4-ms gap must also have exhibited a significant excitatory response following the onset of either the 2-or 8-ms gap, following the criterion established by (Walton et al. 2008). We used the Kolmogorov-Smirnov goodness-of-fit hypothesis test to compare latency distributions, the χ^2 test to compare percentages of cells responsive under differing conditions, and the Wilcoxon rank-sum test to compare tuning widths. A significance criterion of $P < 0.05$ was established for each of these tests before the analyses were performed. We calculated Pearson correlation coefficients to compare tuning within and between tetrodes. All statistical tests were carried out in MATLAB (R2015b; The MathWorks).

Histology. All brains were sectioned coronally. We verified that optic fibers and recording tetrodes accurately targeted auditory cortex using the structure of the hippocampus and the rhinal fissure as rostrocaudal and dorsoventral landmarks (section thickness 100 μm).

RESULTS

We isolated and characterized responses from 627 neurons in the auditory cortex of 9 PV-ChR2 mice. Of these, 187 neurons (30%) responded with short-latency spiking to 100-ms pulses of blue laser light, indicating that they were PV+ interneurons (Lima et al. 2009; Moore and Wehr 2013). PV+ cells generally responded to light in two distinct ways, with either a transient response (Fig. 1*A*, *left*) or a sustained response (Fig. 1*A*, *right*). To investigate these differences further, we separated "transient" from "sustained" neurons (Fig. 1*B*) by comparing their firing within the first 25 ms of photostimulation to firing within the third 25-ms period of photostimulation (Fig. 1*B* shows the log of this ratio). Cells showing sustained responses (Fig. 1*B*; 162 of 187 PV+ cells, or 87%) generally had log ratio values around 0 (i.e., their firing remained roughly constant), whereas transient neurons (Fig. 1*B*; 13%) showed more negative values (after an initially strong response to photostimulation, their firing diminished greatly).

We next looked at the spike waveform for each cell. We found that spike waveforms generally fell into two distinct categories: broad spikes and narrow spikes, similar to previous reports (Kawaguchi and Kubota 1997; Markram et al. 2004;

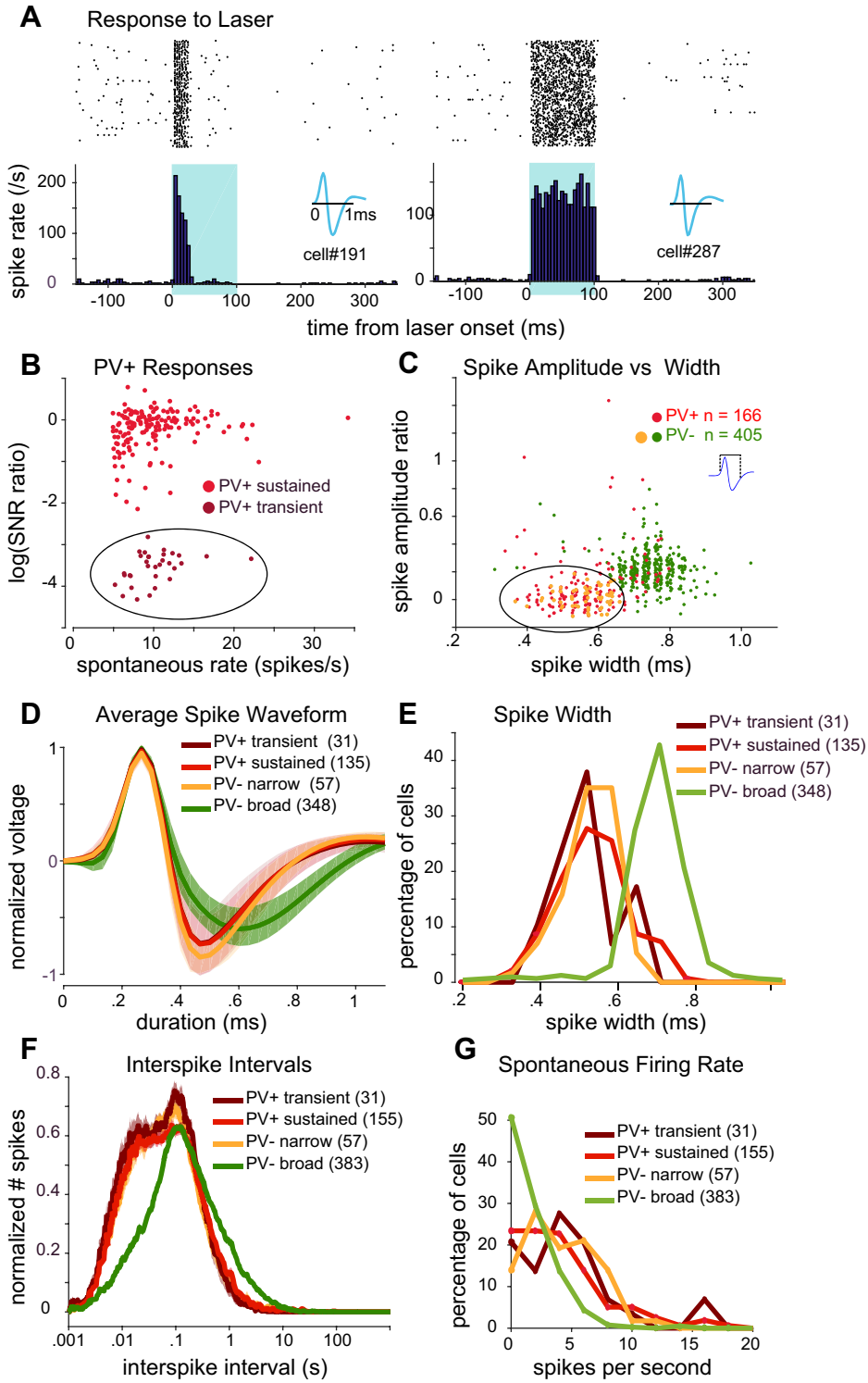

Fig. 1. Identification of cell types. *A*: examples of transient (*left*) and sustained (*right*) parvalbumin-expressing (PV+) responses to laser. Raster plot (*top*) is summarized as a peristimulus time histogram (*bottom*). Illumination (100 ms) is indicated by blue shading. *Insets* show spike waveform of each cell. *B*: for each PV+ cell, the persistence of spiking throughout the duration of the laser pulse is plotted against the cell's spontaneous spike rate. "Persistence" is quantified as the log [signal-to-noise-ratio (SNR) for the third 25-ms period after laser onset divided by SNR for the first 25 ms after laser onset]. We clustered PV+ cells into 2 subsets: transient (dark red circles within ellipse) and sustained (light red circles). *C*: spike peak-to-trough amplitude ratio plotted against peak-to-trough width. *Inset* shows how spike width was measured. A subset of narrow-spiking PV− cells (PV− narrow; orange circles within ellipse) that overlapped with the main cluster of PV+ cells was identified for further analysis. *D*: average spike waveform (solid lines indicate mean across cells, lighter shading denotes SE) for each of the identified cell types. Each cell's average waveform was normalized before averaging across cells. *E*: distribution of spike widths for each cell type. In *C–E*, only cells with spikes recorded with a leading positive phase were included for analysis. *F*: average interspike interval histogram (solid lines indicate mean, lighter shading denotes SE) for each cell type. Histograms were normalized for each cell before averaging. *G*: histograms of spontaneous firing rate for each cell type. Number of cells (in parentheses in *D–G*) for each analysis varied slightly after screening for insufficient data.

Moore and Wehr 2013). As expected from previous work, nearly all transient and sustained PV+ cells had narrow spikes. Most PV− cells fired broad spikes, but a subset (13%) had narrow spikes. Thus we initially examined four categories of cells (transient PV+, sustained PV+, broad-spiking PV−, and narrow-spiking PV−) to determine if they had any further distinguishing characteristics. Figure 1*C* shows the spike amplitude ratio (ratio of the magnitudes of the spike peak and trough) plotted against the spike width. Consistent with previous reports, PV+ interneurons of both the transient and sustained subgroups had relatively short-duration spikes (Fig. 1, *B–E*), with a mean spike width of 0.55 ± 0.015 and 0.57 ± 0.008 ms (means ± SE), respectively (Fig. 1, *C–E*). In contrast, the majority of cells unresponsive to photostimulation showed broader spikes (383 PV− "broad," 61% of total cells), with a mean spike width of 0.74 ± 0.004 ms. Figure 1*C*, however, shows that a subset of PV− neurons (57 PV− "narrow," 9% of total cells) had narrow spike widths (0.56 ± 0.009 ms) similar

to those of PV+ interneurons. The average spike waveform for each category of cell (Fig. 1*D*) demonstrates the clear similarity of waveforms between PV+ sustained, PV+ transient, and PV− narrow putative cell types and their separation from the average waveform of the PV− broad cell type.

PV+ interneurons are also known as "fast-spiking" cells because of their capacity for short-latency responses and sustained high spike rates (Markram et al. 2004). Average interspike interval histograms for each cell type (Fig. 1*F*) and plots of their spontaneous firing rates (Fig. 1*G*) show that PV+ sustained, PV+ transient, and PV− narrow cells all fired at similarly high rates compared with PV− broad cells. In summary, we found no response differences between transient and sustained PV+ cells (other than their response to light). Similarly, when we compared the sound-evoked responses (to WN bursts or gaps in noise) of these two subcategories of PV+ cells, we found that they were indistinguishable (as described below). Therefore, in all subsequent figures, we pool transient and sustained PV+ interneurons into a single PV+ group. In contrast, PV− narrow and PV− broad cell types were clearly differentiable in both their firing properties and their responses to WN bursts and to gaps in noise, and we therefore plot them separately in the figures to follow. Indeed, apart from being nonresponsive to light, PV− narrow cells were nearly indistinguishable from PV+ cells in both their firing properties and their sound-evoked responses.

Gap encoding. We presented mice with continuous white noise that was periodically interrupted by brief gaps ranging in duration from 1 to 256 ms (in octave steps), as well as a control condition without a gap. Most neurons responded with a brief burst of spikes both at the sound offset (start of the gap) and at sound onset (gap termination). Figure 2*A* shows an example of a PV+ neuron responding to gaps. Each horizontal panel shows the response to one gap duration (indicated at *left*). Sound offsets and onsets are denoted, with responses aligned to sound onset (gap termination). Excitatory response windows (50-ms duration) are color-coded for off-responses and on-responses. For this cell, both 128- and 256-ms gaps evoked robust and separable excitatory responses to both sound offset and sound onset. Figure 2*B* shows the gap duration tuning curve for this cell, based on spike counts within each response window. Responses that were significantly different from the "no gap" firing rate ($P < 0.05$, paired *t*-test) are indicated. Although both off- and on-responses were robust and separable at long gap durations, for gaps ≤64 ms these responses overlapped in time so that for shorter gaps it is not possible to assign spikes as having been evoked by offset or onset. However, spikes following sound onset have been shown to play a role in gap detection behavior (Weible et al. 2014b), and thus, for shorter gap stimuli (<32 ms), we report these spikes following sound onset with the understanding that they may result from both sound offset and onset. This cell had significant on-responses for all durations ≥4 ms. This cell also showed a prominent suppression of spiking following the on-response (analyzed in a 70- to 140-ms window after sound onset; Fig. 2*B*).

Both PV+ and PV− narrow cells were more responsive to gaps than were PV− broad cells. A higher percentage of PV+ and PV− narrow cells showed significant responses to at least one gap duration (Fig. 2*C*) compared with PV− broad cells. Excitatory responses to sound offset for 256-ms gaps (for which responses to offset and onset could be clearly discriminated) were significantly more common for PV+ and PV− narrow cells (PV+ vs. PV− broad: $P = 0.0002$, PV− narrow vs. PV− broad: $P = 0.0003$, χ^2 test). Cells showing suppression following these excitatory responses were less common overall, but still more common among PV+ and PV− narrow cells (PV+ vs. PV− broad: $P = 0.005$). Many more cells of all three cell classes showed responses to sound onset (Fig. 2*C*, *right*). As with responses to sound offset, a higher percentage of PV+ and PV− narrow cells showed significant excitatory and suppressive responses to sound onset (excitation: PV+ vs. PV− broad: $P = 0.007$, PV− narrow vs. PV− broad: $P = 0.02$; suppression: PV+ vs. PV− broad: $P < 0.00001$, PV− narrow vs. PV− broad: $P < 0.00001$).

Considering cells with significant responses to brief gaps in noise, PV+ and PV− narrow cells showed a more strongly modulated response than did PV− broad cells. Population-averaged responses to gaps of 256 ms (Fig. 2*D*, *top*) clearly showed strong off- and on-responses and some degree of suppression for all three cell types. However, whereas PV+ and PV− narrow cells showed very similar, deeply modulated response profiles, PV− broad cells showed relatively weaker off- and on-responses and negligible suppression following the on-response. For shorter gaps (8 ms; Fig. 2*D*, *bottom*), off- and on-responses overlapped in time but showed much the same between-cell class pattern as for responses to longer gaps.

For all three cell types, the latencies of firing in response to gaps were broadly distributed across cells. However, PV+ and PV− narrow cells had significantly shorter latencies to sound onset (Fig. 2*E*, *right*) than did PV− broad cells ($P < 0.01$, Kolmogorov-Smirnov goodness-of-fit hypothesis test). Laten-

Fig. 2. Parvalbumin-expressing (PV+) cells show more deeply modulated gap responses. *A*: raster plots and peristimulus time histograms (PSTHs) for an example PV+ cell's responses to gaps (delimited by red vertical lines) with durations of 1–256 ms (red numbers at *left*), aligned to gap termination. Red shading indicates the excitatory "off-response" analysis window; green indicates the excitatory "on-response" analysis window. *B*: gap duration tuning curve of the cell shown in *A* for off-responses (red), on-responses (green), and a window 70–140 ms following the on-response where suppression is often seen (blue). Closed circles indicate significant differences from spontaneous firing rate (dotted line). Off-responses are only shown for gaps ≥32 ms where they are separable from on-responses. *C*: following sound offset (*left*; only 256-ms gaps) or sound onset (*right*; all gap durations), percentage of each cell type showing significant excitatory responses within 0–50 ms and/or suppressive responses from 70 to 140 ms. Brackets above histograms indicate significant differences ($P < 0.05$, χ^2 test). *D*: population-averaged PSTHs for each cell type to a 256-ms gap (*top*) or 8-ms gap (*bottom*), compiled from all cells with a significant (excitatory) response to any gap duration. All cells with significant responses were included (no. of cells in parentheses). Shading denotes SE. Black horizontal bar denotes white noise background; red vertical lines indicate gap beginning and end. Before averaging, a cell's PSTH with spontaneous level subtracted was normalized to its maximum response across all gap durations. *E*: PV+ and PV− narrow cells had shorter response latencies for gaps in noise. We measured latencies as time from sound offset (*left*) or sound onset (*right*) to half peak height for 128- and 256-ms gaps (combined) and smoothed with Gaussian convolution ($\sigma = 5$ ms). All cells with significant responses and peak responses within 128 ms of sound offset (or onset) were included. *F*: for each cell type and each gap duration, the mean (±SE) excitatory on-response (0–50 ms after sound onset) is plotted against postresponse suppression (70–140 ms after sound onset). Lightly shaded arrows show the trajectory of change in the means as gap duration lengthens. For reference, the off-responses for 256-ms gaps are shown with dotted lines (with excitatory response and suppression calculated similarly as for on-responses).

cies to sound offset for all three cell types were broadly distributed (Fig. 2*E*, *left*).

Figure 2*F* summarizes how on-responses change with gap duration, illustrating the deeper modulation of PV+ and PV− narrow cells. The excitatory on-responses (*y*-axis) are plotted against the suppressive responses (*x*-axis) for each cell class and each gap duration. Gaps of only 1 or 2 ms elicit weak excitatory on-responses with no following suppression in all three cell classes. Gap durations of 4 or 8 ms already show stronger excitation of PV+ and PV− narrow cells, but still little or no suppression. With gap durations of 16 ms or longer, PV+ and PV− narrow cells show increasing suppression and a plateaued excitatory response, where PV− broad cells reach a slightly lower peak response

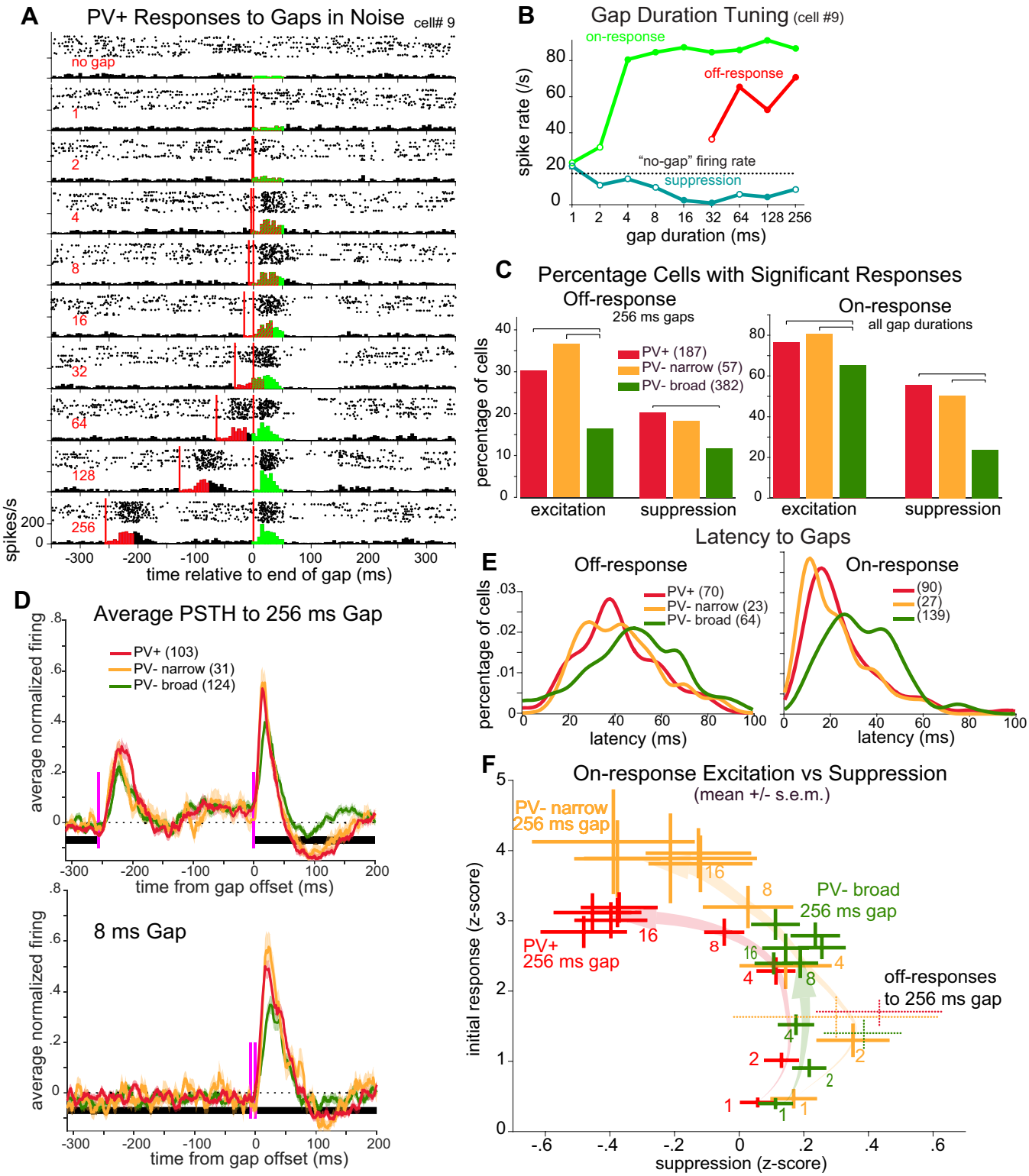

without suppression. The strongest excitatory responses belong to the PV− narrow cell class.

Across the population, a significantly higher percentage of PV+ and PV− narrow cells responded to short gaps (Fig. 3*A*). Similarly, PV+ and PV− narrow cells had shorter preferred gap durations than PV− broad cells (Fig. 3*B*). Previous studies have shown that PV+ cells are more broadly tuned than PV− cells for some stimulus features, such as orientation (in mouse visual cortex), but not for other features, such as frequency (in auditory cortex) (Kerlin et al. 2010; Moore and Wehr 2013). This is thought to arise from local pooling of inputs by PV+ cells and thus to depend on whether neurons in the local neighborhood show heterogenous tuning (as they do for orientation) or similar tuning (as they do for frequency). To examine this for gap duration tuning, we first measured tuning width. For each cell, we aligned the gap duration tuning curve to the preferred gap duration and then computed population-averaged tuning curves. We found that PV+ cells were slightly but significantly more broadly tuned to gap duration than PV− broad cells [Fig. 3*C*; width at half-height: 3.5 octaves (PV+) vs. 2.9 octaves (PV− broad), $P = 0.014$, rank-sum test]. To examine whether gap duration tuning of neighboring neurons is similar or heterogeneous, we asked whether the preferred gap duration of a given cell had any predictive value about the preferred duration of neighboring cells recorded on the same tetrode. Preferred gap duration was uncorrelated with that of neighboring cells ($r = 0.03$, $P = 0.84$, $n = 39$ simultaneously recorded cells), suggesting that gap duration tuning is heterogeneous among the local population.

Noise burst encoding. Are these response differences among cell classes specific to gaps, or are they general features of on- and off-responses? To test the generality of on- and off-responses for different cell classes, we presented each cell with WN bursts of varying duration (1–256 ms, in octave steps). Overall, responses to gaps in noise and to WN bursts were quite similar for each cell class despite the difference in temporal structure of the two stimulus types. Latency distributions revealed faster response times for PV+ and PV− narrow cells compared with PV− broad cells (Fig. 4*A*; $P < 0.01$, Kolmogorov-Smirnov goodness-of-fit hypothesis test). Significantly more PV+ and PV− narrow cells showed excitatory responses to sound onsets (Fig. 4*B*, *left*; $P < 0.05$, χ^2 test) when all burst durations were considered. Similarly, more PV+ and PV− narrow cells showed excitatory responses to sound offsets when only longer (128 and 256 ms) durations were considered in which sound onset and sound offset responses were clearly separable (Fig. 4*B*, *right*; $P < 0.05$, χ^2 test). For each duration tested, we found a significantly greater proportion of PV+ and PV− narrow cells to be responsive to sound onsets (Fig. 4*C*, *left*) compared with PV− broad cells. Suppressive responses following the initial excitatory response were also significantly more common in PV+ and PV− narrow cells (Fig. 4*C*, *right*) for longer (128 and 256 ms) burst durations.

We found that PV+ and PV− narrow cells had higher spontaneous firing rates than PV− broad cells (Fig. 1*G*) and also that they showed stronger and more prevalent suppressive responses (Fig. 4*B*). We wondered whether the stronger suppression we observed for PV+ cells could be a trivial consequence of the higher spontaneous rate, because suppression can only be detected as a reduction below the spontaneous rate. To test this, we used an analysis of covariance to ask how the strength of suppression depended on spontaneous firing rate and cell type. In addition to significant effects of cell type ($F = 17$, $P = 3.9 \times 10^{-5}$) and spontaneous rate ($F = 178$, $P = 1.7 \times 10^{-35}$), we found that there was a significant interaction

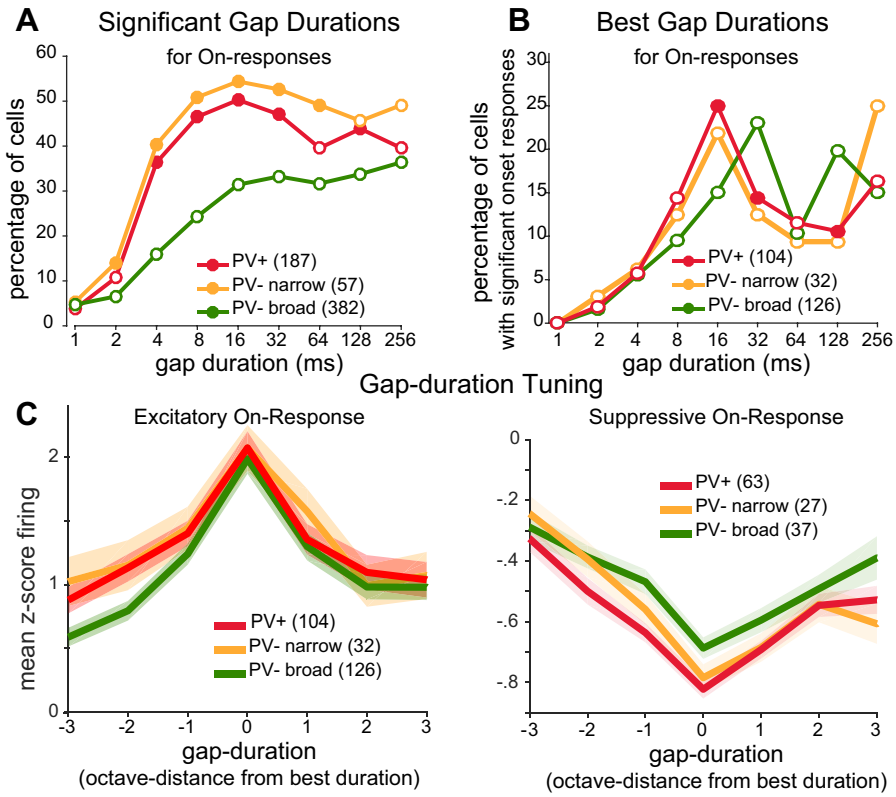

Fig. 3. Tuning of on-responses to gap duration for each cell class. *A*: percentage of cells with significant on-responses to each gap duration (closed circles: $P < 0.05$ significantly different from PV− broad, χ^2 test). B) Distribution of best gap durations for cells that had significant on-responses (filled circles: $P < 0.10$ significantly different from PV− broad, χ^2 test). *C*: population-averaged gap duration tuning curves. Duration tuning curves for excitatory (*left*) or suppressive (*right*) responses were aligned to each cell's best gap duration (solid lines indicate mean; shaded area denotes SE). Baseline firing rates correspond to *z* scores of zero. Gap durations are represented in octaves from best gap duration (i.e., in $\log_2$ units of the duration in ms).

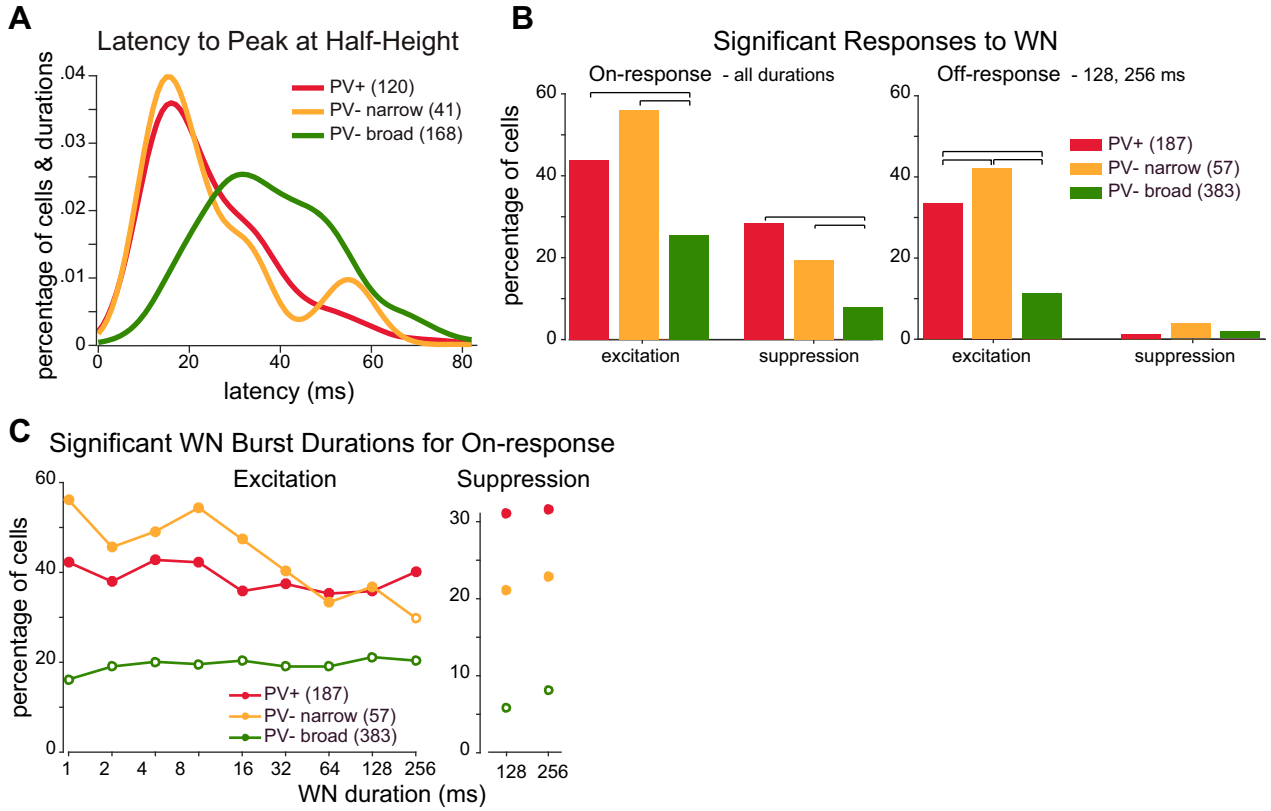

Fig. 4. Responses to white noise (WN) bursts. *A*: latency from stimulus onset to the time when firing first reached half the height of the peristimulus time histogram peak. Latencies were compiled across cells and burst durations with significant responses. *B*: percentage of cells with significant on-responses (*left*) or off-responses (*right*) to WN bursts to any of the tested durations. Brackets above histograms indicate significant differences ($P < 0.05$, χ^2 test). *C*: percentage of cells with significant excitatory (*left*) or suppressive (*right*) on-responses for each burst duration (closed circles indicate significant difference from PV− broad cell response, $P < 0.05$, χ^2 test).

between cell type and spontaneous rate ($F = 32$, $P = 1.9 \times 10^{-8}$), indicating that the stronger suppression seen in PV+ cells is cell-type specific and not simply explained by their higher spontaneous rate.

As with responses to gaps in noise, population-averaged responses to WN bursts were more strongly modulated for PV+ and PV− narrow cells than for PV− broad cells (Fig. 5*A*). Responses to sound onset and offset were easily separable during 256-ms WN bursts (Fig. 5*A*, *left*), and the population-averaged responses of PV+ and PV− narrow were quite similar to each other. They each showed stronger excitatory responses to both sound onset and sound offset than did PV− broad cells. PV+ cells showed significant suppression following the excitatory response to sound onset, whereas PV− narrow cells showed weaker suppression, and PV− broad cells showed no suppression. On- and off-responses began to merge as the burst duration shortened. At intermediate durations (Fig. 5*A*, *middle*), temporal summation of on-evoked suppression with off-evoked excitation appeared to weaken PV+ responses more than it did PV− narrow responses. At short burst durations (4 ms; Fig. 5*A*, *right*), responses of PV+ and PV− narrow cells were indistinguishable, with strong excitatory responses followed by weak suppression. By comparison, PV− broad responses were much weaker.

Despite the differences between cell classes in the percentage of cells with significant excitatory responses to burst offset, all three cell classes had similarly broad distributions of "best" excitatory durations (Fig. 5*B*). Tuning width for noise bursts was no different across cell types (Fig. 5*C*; $P > 0.10$, rank-sum test). Preferred burst duration for a given cell was uncorrelated with that of neighboring cells recorded on the same tetrode ($r = -0.05$, $P = 0.76$, $n = 35$).

DISCUSSION

In this study we recorded from PV+ interneurons in auditory cortex to determine how they encode gaps in noise, a model of temporal processing more generally. We found that, in response to gaps, PV+ cells have stronger and more prevalent on-responses, off-responses, and postresponse suppression compared with PV− cells with broad spikes, which we presume to be pyramidal neurons (PNs). We summarize this pattern of differences as "deeper modulation" of gap responses in PV+ cells. Compared with PNs, PV+ cells were more likely to respond to short gaps and had shorter preferred gap durations. Response latencies were also markedly faster for PV+ cells, consistent with previous findings (Atencio and Schreiner 2008; Moore and Wehr 2013). We found a similar pattern of deeper modulation and faster latencies for responses to WN bursts, suggesting that these are general properties of on- and off-responses in PV+ cells rather than specific features of gap encoding. These findings are consistent with a role for PV+ cells in providing dynamic gain control by pooling local activity. Although gain control is important for temporal processing, these results argue against any specialized role of PV+ cells in gap detection.

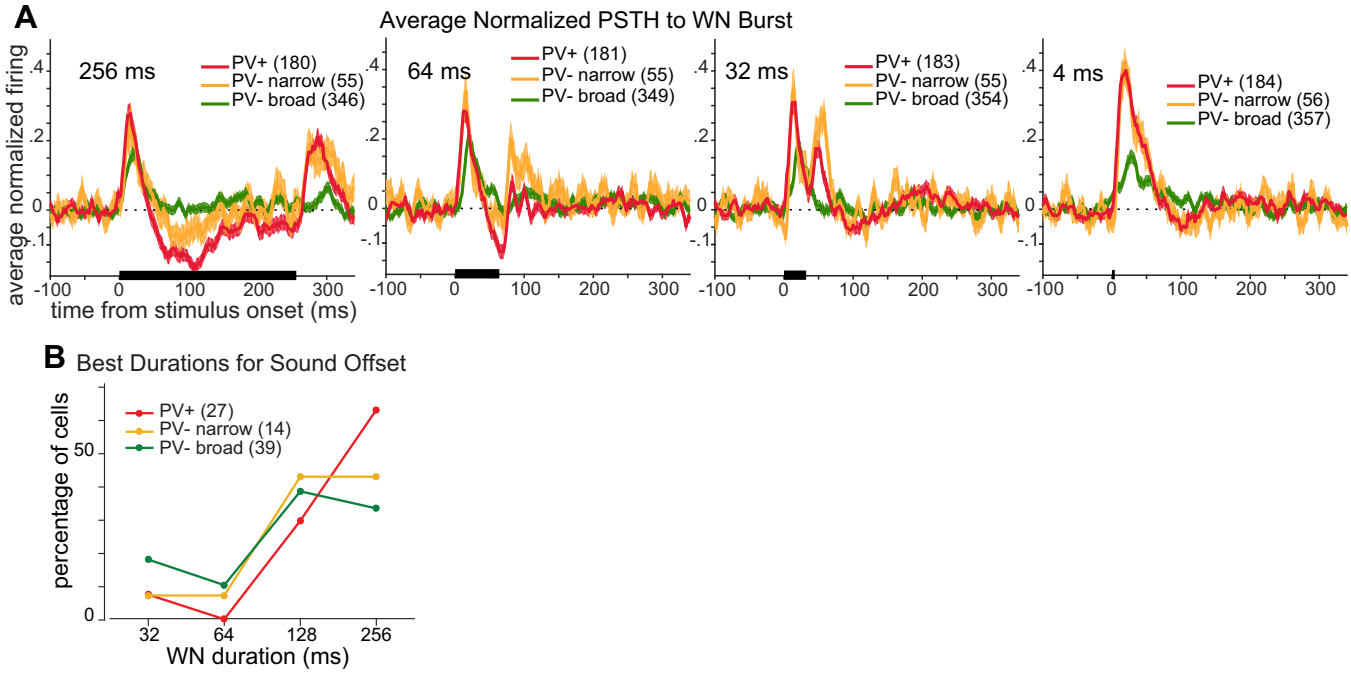

Fig. 5. Tuning of responses to white noise (WN) burst duration. *A*: normalized poststimulus time histograms (PSTH) to WN bursts averaged across cells that showed significant responses (shaded area denotes SE) to this burst duration. Four burst durations are shown (duration is shown at *top left* of each panel). The stimulus is indicated by the black horizontal bar. *B*: distribution of best durations for cells with significant excitatory responses to burst offset. Note that responses to durations ≤32 ms include spikes evoked by both sound onset and offset. Responses to 32- and 64-ms bursts include both excitatory responses and suppressive responses evoked by sound onset. Responses to 128- and 256-ms bursts include only off-responses. The percentages of cells responding to a given duration were not significantly different across cell types (all $P > 0.05$, χ^2 test).

Synaptic inhibition has been proposed to play a number of functional roles in temporal processing. On the basis of effects of optogenetic manipulations on gap detection behavior, we recently proposed a model in which cortical inhibitory interneurons contribute to gap detection by performing a temporal comparison between ongoing and recent cortical activity (Weible et al. 2014b). This model predicts that gap responses of inhibitory interneurons should resemble low-pass filtered responses of PNs; that is, interneuron gap responses should be slower and more prolonged than those of PNs. The gap responses of PV+ cells are clearly inconsistent with this model, because they had faster latencies than PNs and had population responses no more prolonged than those of PNs. More generally, inhibition has been proposed to sculpt the tuning of target cells by suppressing responses to nonpreferred stimuli. Although we found that PV+ cells were tuned for specific gap durations, we found no evidence to support the idea that they confer gap duration tuning to PNs. The preferred gap duration of a PV+ cell had no predictive value about the tuning of neighboring PNs recorded on the same tetrode.

PV+ cells have been widely proposed to provide dynamic gain control for the cortical network by nonselectively pooling input from local excitatory neurons (Atallah et al. 2012; Hofer et al. 2011; Kerlin et al. 2010; Moore and Wehr 2013). PV+ cells receive dense input from nearby excitatory cells (Thomson and Lamy 2007), and their tuning for stimulus features approximates the average tuning of the local network. Thus PV+ cells in auditory cortex are well tuned for frequency, because local neurons share similar frequency tuning, whereas PV+ cells in visual cortex are quite broadly tuned for orientation, because they average across local neurons with heterogenous orientation tuning (Hofer et al. 2011; Kerlin et al. 2010; Moore and Wehr 2013; Zariwala et al. 2011). We found that PV+ cells were slightly but significantly more broadly tuned for gap duration than PV− cells. This result is consistent with local pooling by PV+ cells, which therefore predicts that the preferred gap duration tuning of local excitatory cells should be heterogeneous. Indeed, we found that the preferred gap duration of a given cell had no predictive value about the tuning of neighboring cells recorded on the same tetrode. Together with a growing body of work in visual, somatosensory, and auditory cortex, these results suggest that PV+ neurons pool input from the local network, consistent with a role in providing dynamic gain control. We found that PV+ cells respond faster and more strongly to transient inputs than presumed PNs, indicating that the gain control they provide is both rapid and powerful, in striking contrast to the slower timescale of adaptation that would be involved in a temporal comparison between ongoing and recent cortical activity.

We found that PV+ cells (and PV− cells with narrow spikes) had markedly faster response latencies than PNs, as well as stronger and more prevalent driven responses, and that these were true for responses to either gaps or noise bursts. These findings agree with previous studies of PV+ and fast-spiking cells and likely arise from both faster membrane time constants (Cardin et al. 2007) as well as powerful thalamocortical and intracortical synaptic drive (Hofer et al. 2011; Swadlow 2003). Although we did not measure the frequency tuning of PV+ cells in this study, previous work has shown that they have similar width of spectral tuning as non-PV cells (Moore and Wehr 2013), indicating that their greater sensitivity to broadband stimulus transients is not explained by broader spectral tuning. Rather, these response properties appear to be general features of PV+ cells and suggest that they are opti-

mized for the rapid detection of stimulus transients and thereby provide rapid feedforward inhibition to PNs. This fast and powerful inhibition has been shown to enhance the temporal precision and reliability of PN spiking in auditory cortex (Wehr and Zador 2003). Such precise and reliable spiking responses have a considerable impact on gap detection, because gap responses in auditory cortex make a critical contribution to the perceptual detection of brief gaps (Weible et al. 2014b).

We found that PV+ cells had narrow spike waveforms compared with PV− cells, although the spike width distributions were partially overlapping, in agreement with previous work (Atencio and Schreiner 2008; Moore and Wehr 2013; Niell and Stryker 2008; Runyan et al. 2010; Wu et al. 2008). A small subset of PV− cells (13%) also had narrow spikes, and these cells were indistinguishable from PV+ cells in every aspect we tested (both sensory and biophysical). Thus the meaningful categories in this study were narrow-spiking cells (PV+ and PV−) and broad-spiking cells (PV−, presumed PNs). The identity of PV− narrow-spiking cells is not clear, although it is possible that they are PV− basket cells, which might express somatostatin (for review, see Markram et al. 2004; Yavorska and Wehr 2016). Although no previous studies have investigated gap encoding in inhibitory neurons (whether identified genetically or by spike waveform), it is important to note that previous findings have not always agreed about frequency tuning width (Atencio and Schreiner 2008; Li et al. 2015; Moore and Wehr 2013). Those differences are likely due to laminar differences and to the genetic or waveform criteria used to categorize cells, and could very likely be influenced by anesthesia. A strength of the chronic tetrode approach we used is that it permits recordings from awake mice, but a limitation is the lack of reliable laminar depth information. These factors will be important to consider comparing with future work.

We found that late, sound-evoked suppression was stronger in PV+ and PV− narrow cells than in PV− broad cells. The latency of this suppression was too long for it to affect the initial, excitatory gap responses of PV+ or other cells, but it could affect temporal processing for more prolonged or repetitive signals (such as amplitude-modulated noise, click trains, or prolonged natural sounds). This suppression could be caused by synaptic depression following the synaptic release that drives excitatory responses (Wehr and Zador 2005). Alternatively, it could be due to network suppression mediated by somatostatin-expressing interneurons originating from distant frequency-tuned areas that are activated by the white noise transients (Kato et al. 2017). This suppression may not be evident in recordings from anesthetized animals, which generally show low levels of spontaneous activity, because suppression may only be revealed by high spontaneous rates typically seen in awake animals. This suppression could enhance signal-to-noise in either the temporal domain or the spectral domain, which could be especially important for the processing of temporally or spectrally complex signals.

The picture that emerges from these results is that PV+ cells are optimized to encode rapid stimulus transients and thereby play a fundamental role in controlling the gain and timing of cortical spiking responses. This appears to be generally true for responses to gaps in noise, noise bursts, tones, and other sounds. Thus, despite the absence of any specific role in gap detection, PV+ cells clearly have a great impact on temporal processing. A loss of PV+ cells or a reduction in their synaptic efficacy would be expected to lead to a corresponding loss of dynamic gain control and temporal precision, which would in turn cause deficits in temporal processing in general and gap detection in particular. A growing body of work has shown that hearing loss reduces cortical inhibitory function, whether due to acoustic trauma, conductive hearing loss, or age (Caspary et al. 2008; Martin del Campo et al. 2012; Scholl and Wehr 2008; Takesian et al. 2012). It seems plausible that these effects, and the resulting deficits in gap detection and speech comprehension, could be mediated specifically by impairments to PV+ cell function.

GRANTS

This work was supported by National Institute on Deafness and Other Communication Disorders Grant R01 DC-015828.

DISCLOSURES

No conflicts of interest, financial or otherwise, are declared by the authors.

AUTHOR CONTRIBUTIONS

M.W. conceived and designed research; C.H.K. and K.K. performed experiments; C.H.K., K.K., and M.W. analyzed data; C.H.K. and M.W. interpreted results of experiments; C.H.K. prepared figures; C.H.K. and M.W. drafted manuscript; C.H.K. and M.W. edited and revised manuscript; C.H.K. and M.W. approved final version of manuscript.

REFERENCES

Atallah BV, Bruns W, Carandini M, Scanziani M. Parvalbumin-expressing interneurons linearly transform cortical responses to visual stimuli. *Neuron* 73: 159–170, 2012. doi:10.1016/j.neuron.2011.12.013.

Atencio CA, Schreiner CE. Spectrotemporal processing differences between auditory cortical fast-spiking and regular-spiking neurons. *J Neurosci* 28: 3897–3910, 2008. doi:10.1523/JNEUROSCI.5366-07.2008.

Ben-David BM, Chambers CG, Daneman M, Pichora-Fuller MK, Reingold EM, Schneider BA. Effects of aging and noise on real-time spoken word recognition: evidence from eye movements. *J Speech Lang Hear Res* 54: 243–262, 2011. doi:10.1044/1092-4388(2010/09-0233).

Cardin JA, Palmer LA, Contreras D. Stimulus feature selectivity in excitatory and inhibitory neurons in primary visual cortex. *J Neurosci* 27: 10333–10344, 2007. doi:10.1523/JNEUROSCI.1692-07.2007.

Caspary DM, Ling L, Turner JG, Hughes LF. Inhibitory neurotransmission, plasticity and aging in the mammalian central auditory system. *J Exp Biol* 211: 1781–1791, 2008. doi:10.1242/jeb.013581.

Fitzgibbons PJ, Gordon-Salant S. Auditory temporal processing in elderly listeners. *J Am Acad Audiol* 7: 183–189, 1996.

Glasberg BR, Moore BC, Bacon SP. Gap detection and masking in hearing-impaired and normal-hearing subjects. *J Acoust Soc Am* 81: 1546–1556, 1987. doi:10.1121/1.394507.

Helfer KS, Vargo M. Speech recognition and temporal processing in middle-aged women. *J Am Acad Audiol* 20: 264–271, 2009. doi:10.3766/jaaa.20.4.6.

Hofer SB, Ko H, Pichler B, Vogelstein J, Ros H, Zeng H, Lein E, Lesica NA, Mrsic-Flogel TD. Differential connectivity and response dynamics of excitatory and inhibitory neurons in visual cortex. *Nat Neurosci* 14: 1045–1052, 2011. doi:10.1038/nn.2876.

Ison JR, Allen PD, O'Neill WE. Age-related hearing loss in C57BL/6J mice has both frequency-specific and non-frequency-specific components that produce a hyperacusis-like exaggeration of the acoustic startle reflex. *J Assoc Res Otolaryngol* 8: 539–550, 2007. doi:10.1007/s10162-007-0098-3.

Kato HK, Asinof SK, Isaacson JS. Network-level control of frequency tuning in auditory cortex. *Neuron* 95: 412–423.e4, 2017. doi:10.1016/j.neuron.2017.06.019.

Kawaguchi Y, Kubota Y. GABAergic cell subtypes and their synaptic connections in rat frontal cortex. *Cereb Cortex* 7: 476–486, 1997. doi:10.1093/cercor/7.6.476.

Kerlin AM, Andermann ML, Berezovskii VK, Reid RC. Broadly tuned response properties of diverse inhibitory neuron subtypes in mouse visual cortex. *Neuron* 67: 858–871, 2010. doi:10.1016/j.neuron.2010.08.002.

Li LY, Xiong XR, Ibrahim LA, Yuan W, Tao HW, Zhang LI. Differential receptive field properties of parvalbumin and somatostatin inhibitory neurons in mouse auditory cortex. *Cereb Cortex* 25: 1782–1791, 2015. doi:10.1093/cercor/bht417.

Lima SQ, Hromádka T, Znamenskiy P, Zador AM. PINP: a new method of tagging neuronal populations for identification during in vivo electrophysiological recording. *PLoS One* 4: e6099, 2009. doi:10.1371/journal.pone.0006099.

Markram H, Toledo-Rodriguez M, Wang Y, Gupta A, Silberberg G, Wu C. Interneurons of the neocortical inhibitory system. *Nat Rev Neurosci* 5: 793–807, 2004. doi:10.1038/nrn1519.

Martin del Campo HN, Measor KR, Razak KA. Parvalbumin immunoreactivity in the auditory cortex of a mouse model of presbycusis. *Hear Res* 294: 31–39, 2012. doi:10.1016/j.heares.2012.08.017.

Moore AK, Wehr M. Parvalbumin-expressing inhibitory interneurons in auditory cortex are well-tuned for frequency. *J Neurosci* 33: 13713–13723, 2013. doi:10.1523/JNEUROSCI.0663-13.2013.

Niell CM, Stryker MP. Highly selective receptive fields in mouse visual cortex. *J Neurosci* 28: 7520–7536, 2008. doi:10.1523/JNEUROSCI.0623-08.2008.

Runyan CA, Schummers J, Van Wart A, Kuhlman SJ, Wilson NR, Huang ZJ, Sur M. Response features of parvalbumin-expressing interneurons suggest precise roles for subtypes of inhibition in visual cortex. *Neuron* 67: 847–857, 2010. doi:10.1016/j.neuron.2010.08.006.

Schneider BA, Pichora-Fuller MK, Kowalchuk D, Lamb M. Gap detection and the precedence effect in young and old adults. *J Acoust Soc Am* 95: 980–991, 1994. doi:10.1121/1.408403.

Scholl B, Wehr M. Disruption of balanced cortical excitation and inhibition by acoustic trauma. *J Neurophysiol* 100: 646–656, 2008. doi:10.1152/jn.90406.2008.

Snell KB, Frisina DR. Relationships among age-related differences in gap detection and word recognition. *J Acoust Soc Am* 107: 1615–1626, 2000. doi:10.1121/1.428446.

Swadlow HA. Fast-spike interneurons and feedforward inhibition in awake sensory neocortex. *Cereb Cortex* 13: 25–32, 2003. doi:10.1093/cercor/13.1.25.

Takesian AE, Kotak VC, Sanes DH. Age-dependent effect of hearing loss on cortical inhibitory synapse function. *J Neurophysiol* 107: 937–947, 2012. doi:10.1152/jn.00515.2011.

Tallal P, Stark RE, Mellits ED. Identification of language-impaired children on the basis of rapid perception and production skills. *Brain Lang* 25: 314–322, 1985. doi:10.1016/0093-934X(85)90087-2.

Thomson AM, Lamy C. Functional maps of neocortical local circuitry. *Front Neurosci* 1: 19–42, 2007. doi:10.3389/neuro.01.1.1.002.2007.

Walton JP. Timing is everything: temporal processing deficits in the aged auditory brainstem. *Hear Res* 264: 63–69, 2010. doi:10.1016/j.heares.2010.03.002.

Walton JP, Barsz K, Wilson WW. Sensorineural hearing loss and neural correlates of temporal acuity in the inferior colliculus of the C57BL/6 mouse. *J Assoc Res Otolaryngol* 9: 90–101, 2008. doi:10.1007/s10162-007-0101-z.

Wehr M, Zador AM. Balanced inhibition underlies tuning and sharpens spike timing in auditory cortex. *Nature* 426: 442–446, 2003. doi:10.1038/nature02116.

Wehr M, Zador AM. Synaptic mechanisms of forward suppression in rat auditory cortex. *Neuron* 47: 437–445, 2005. doi:10.1016/j.neuron.2005.06.009.

Weible AP, Liu C, Niell CM, Wehr M. Auditory cortex is required for fear potentiation of gap detection. *J Neurosci* 34: 15437–15445, 2014a. doi:10.1523/JNEUROSCI.3408-14.2014.

Weible AP, Moore AK, Liu C, DeBlander L, Wu H, Kentros C, Wehr M. Perceptual gap detection is mediated by gap termination responses in auditory cortex. *Curr Biol* 24: 1447–1455, 2014b. doi:10.1016/j.cub.2014.05.031.

Wu GK, Arbuckle R, Liu BH, Tao HW, Zhang LI. Lateral sharpening of cortical frequency tuning by approximately balanced inhibition. *Neuron* 58: 132–143, 2008. doi:10.1016/j.neuron.2008.01.035.

Yavorska I, Wehr M. Somatostatin-expressing inhibitory interneurons in cortical circuits. *Front Neural Circuits* 10: 76, 2016. doi:10.3389/fncir.2016.00076.

Zariwala HA, Madisen L, Ahrens KF, Bernard A, Lein ES, Jones AR, Zeng H. Visual tuning properties of genetically identified layer 2/3 neuronal types in the primary visual cortex of cre-transgenic mice. *Front Syst Neurosci* 4: 162, 2011. doi:10.3389/fnsys.2010.00162.